

# Mesoscale orographic flows

Haraldur Ólafsson<sup>a</sup> and Hálf dán Ágústsson<sup>b,c,d</sup>

<sup>a</sup>School of Atmospheric Sciences, Science Institute, and Faculty of Physical Sciences, University of Iceland, Veðurfélagið and the Icelandic Meteorological Office, Reykjavík, Iceland <sup>b</sup>Kjeller vindteknikk Ltd., Lillestrøm, Norway <sup>c</sup>Belgingur Ltd., Reykjavík, Iceland <sup>d</sup>School of Atmospheric Sciences, Science Institute, University of Iceland, Reykjavík, Iceland

## 1 Introduction

Mountains, and hills are a source of enormous variability in atmospheric flow at a multitude of scales. Variations in direction and speed of the flow, both in time and space, are associated with variations in all parameters that are generally associated with weather forecasting, including wind, temperature, cloudiness, and precipitation. In the vicinity of mountains, climate, weather, and in particular weather extremes may be highly influenced by the topography. In this chapter, a comprehensive, but short review of the impact of mountains on the atmospheric flow will be given and aspects of forecasting the different orographic wind patterns will be discussed.

## 2 Patterns of mountain flows

Atmospheric flow is described by the momentum equation

$$\frac{\partial \mathbf{V}}{\partial t} + \mathbf{V} \cdot \nabla \mathbf{V} = -\frac{1}{\rho} \nabla P - f \mathbf{k} \times \mathbf{V} - g - \frac{\partial(u'w')}{\partial z} - \frac{\partial(v'w')}{\partial z} \quad (1)$$

I            II            III            IV            V            VI            VII

where  $\mathbf{V}$  is the wind vector, with components  $u$ ,  $v$ , and  $w$ ,  $P$  is pressure,  $f$  is the Coriolis parameter, and  $g$  is gravity. Term I represents changes of the wind field in time, term II represents acceleration associated with spatial variability of the wind, term III is the pressure gradient force, term IV is the Coriolis force, term V is the gravity and terms VI and VII represent the turbulent vertical transfer of horizontal momentum.

In order to facilitate the analysis of orographic flows, two nondimensional numbers are defined, the Rossby number, and the nondimensional mountain height, sometimes referred to as the inverse Froude number. Scale analysis of terms II and IV in Eq. (1) yields respectively  $U^2/L$  and  $fU$ . The ratio of these two terms is the Rossby number

$$Ro = U/fL$$

A popular interpretation of the Rossby number is a measure of to what extent the flow is geostrophic. If the Rossby number is far below unity, term IV dominates term II and the flow is close to geostrophic. Another way of formulating an interpretation is whether it is the Coriolis term or the nonlinear terms that act to balance a pressure gradient in frictionless and stationary flow.

Another dimensionless number, referring to energy and associated with the gravity term (V) and the nonlinear terms (II) in Eq. (1) is the nondimensional mountain height or the inverse Froude number

$$Fr^{-1} = Nh/U$$

where  $N$  is the Brunt-Vaisala frequency or the static stability of the airmass,  $h$  represents the vertical distance a particle ascends, or the height of the obstacle on which the flow is impinging, and  $U$  is the flow speed. The  $Nh/U$  may be interpreted as the ratio of the potential energy associated with the stratification of the flow ascending the mountain, and the kinetic energy of the flow.  $Nh/U$  may also be interpreted as a measure of the internal gravity wave speed to the speed of the flow itself.

Patterns of atmospheric flow in the vicinity of a mountain may be classified according to the values of the above dimensionless numbers,  $Ro$  and  $Fr^{-1}$ . The diagram in Fig. 1 shows these patterns schematically. In the upper left corner (high  $Ro$ , low  $Nh/U$ ), there is typically an airmass with low static stability impinging on low obstacles and there is a negligible

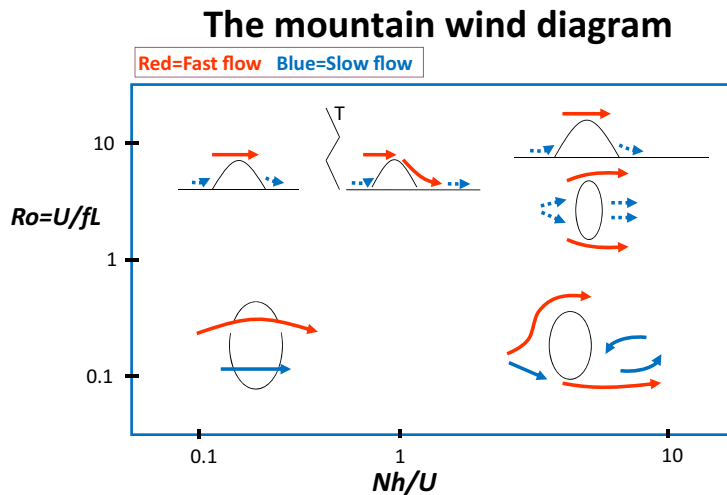


FIG. 1 A diagram of the main patterns of orographic flows, classified according to the values of the dimensionless numbers  $Ro$  and  $Nh/U$ .

impact of the Coriolis force upon the flow pattern. This is often referred to as flow over hills. Such flows are characterized by relatively fast flow on the top of the hills, but weaker flow at lower elevations, in between hills. The flow pattern may be sensitive to surface friction and the shape of the terrain, particularly on the downwind side, where a boundary-layer separation and wake formation may occur. Simulating such a pattern is hard and a true challenge for the parameterization of the numerical models. A review of flow over hills is given in, for instance, [Belcher and Hunt \(1998\)](#).

In the upper middle part of the diagram, there is a celebrated zone of amplified gravity waves and high orographic drag. The flow upstream of the mountain is in general not blocked, except perhaps at the bottom of the boundary-layer. Above the mountain, there are amplified gravity waves that may trail downstream and to some extent laterally. The flow in the gravity wave above the mountain is fast on its way downwards, but slow on its way upwards. Accordingly, the phase lines of the waves tilt upstream with height. The greater the amplitude of the waves are, the stronger is the acceleration in the downward flow. At the surface of the earth, this flow is often referred to as a downslope windstorm. A downslope windstorm may also occur where the waves are not very amplified. In this case, they are considered to break below a critical layer, above which the waves do not penetrate (e.g. [Smith, 1985](#)). Downslope acceleration and subsequent wake formation further downstream may also be described within the shallow water framework, where the flow moves from a subcritical to supercritical state over the mountain, accelerates over the downslopes, after which it decelerates suddenly in a hydraulic jump. The downslope acceleration does indeed occur in ideal, vertically nonstructured flow (e.g., [Durrán, 1990](#); [Ólafsson and Bougeault, 1996](#)), but the downslope acceleration is known to be sensitive to the vertical profile of the flow. Strong wave development is often associated with a stable layer or an inversion and a moderate change in the strength or the position of the inversion may have large impacts on the gravity waves and the downslope flow. Amplification of the waves and strong downslope flow may be enhanced by a positive vertical wind shear, while trapping of the wave energy at low levels, and strong downslope winds may also be favored by a negative vertical wind shear or a directional wind shear. The extent of the downslope windstorms, and the downstream flow pattern in general, is quite variable, ranging from smooth wavy field to well mixed turbulent flow. [Hertenstein and Kuettner \(2005\)](#) have proposed a diagram to classify the downstream flow where the key variables are the vertical wind shear, and the inversion strength. [Ágústsson and Ólafsson \(2010, 2014\)](#) have described two types of strong downslope flow an extended windstorm with no waves downstream, and a windstorm with a short downstream extension, and a wavy downstream flow field. The above papers include references to many articles dealing with different aspects of downslope acceleration.

In short, there is no universal theory of downslope windstorms in vertically nonuniform stratified flow, but in general, strong winds, and statically stable layers, particularly close to mountain top level, favor downslope acceleration. An extensive description of waves and other aspects of stratified and vertically structured flows over obstacles is given in [Baines \(1995\)](#).

In the upper right corner of the diagram in [Fig. 1](#), there is blocked flow with corner/gap winds, and a wake, shown schematically in [Fig. 2](#), and in a high-resolution simulation of real flow in [Fig. 3](#). This is typical for high mountain ranges, and for moderate to low mountain ranges in weak winds. In blocked flows, there is a large area of weak winds upstream of

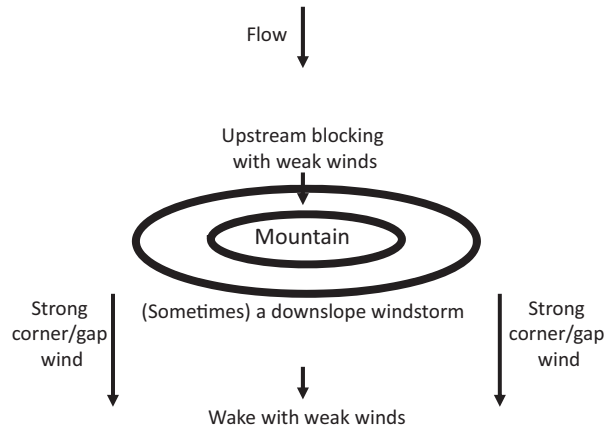


FIG. 2 A schematic of the main patterns of mesoscale orographic flows.

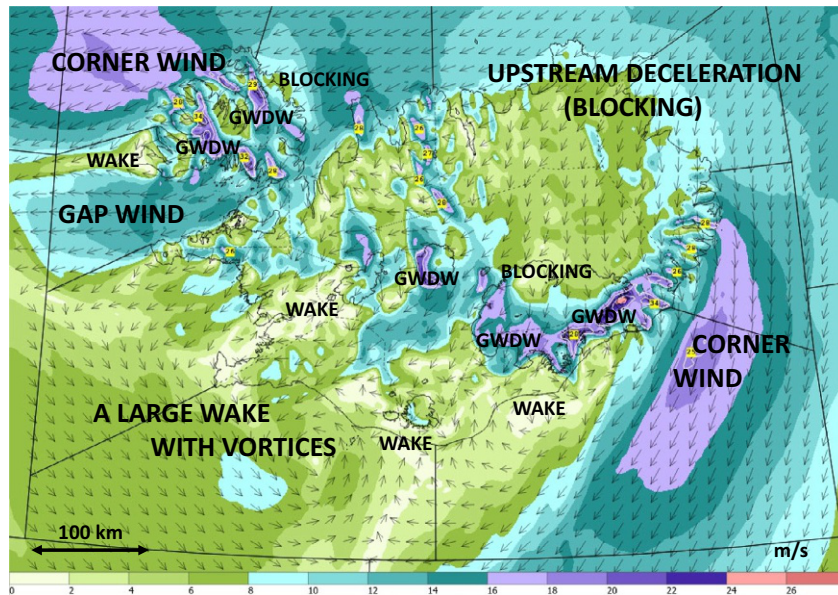


FIG. 3 Wind speed at 10m (m/s) and identification of some of the main elements of mesoscale orographic flows in a case of northeasterly flow over Iceland on 29 June 2020 at 06 UTC. "GWDW" stands for gravity wave and a downslope windstorm. The flow is simulated in real-time by the numerical model Harmonie operated by the Icelandic Meteorological Office and the Danish Meteorological Institute at a horizontal resolution of 2.5 km.

the mountain, called a blocking, and a speed-up where the flow leaves the blocking. There is relatively fast flow at the mountain edges, from which jets may extend large distances. These jets are often referred to as corner winds or gap winds. Barrier winds may blow along the mountain, away from the blocking. A simple way of looking at the dynamics of the blocking is to consider conservation of energy along a streamline approaching the mountain, referring to terms II, III, and V in Eq. (1). This gives, after integration

$$0 = \frac{1}{2}\rho V^2 + P + \rho gz$$

here, the kinetic energy of the flow is redistributed to increased pressure, and increased potential. This happens as the flow meets the mountain, decelerates, ascends, and the pressure increases, relative to the pressure at the same elevation further upstream of the mountain. Traditionally, the term blocking refers to stagnant flow, i.e., that the surface flow is unable to overcome the potential barrier of the mountain, and stagnates. The onset of blocking has been dealt with by many authors, such as [Smith \(1989\)](#) and [Smith and Grønås \(1993\)](#). There may, however, be considerable upstream deceleration on the upstream side, but no blocking, and yet the region of decelerated flow is often referred to as an upstream blocking. On the downstream side of the mountain, there is relatively low pressure, and in flow described by linear theory (which, strictly speaking, refers to the low values of the  $Nh/U$ ), the upstream, and downstream pressure anomalies are symmetric, but with opposite signs ([Smith, 1989](#)). The associated horizontal pressure gradient drives the corner or gap winds, and such winds have been investigated, and described by many authors, such as [Ólafsson and Bougeault \(1996\)](#), [Zängl \(2002\)](#), [Gaberšek and Durran \(2004, 2006\)](#), and others.

The orographic wake is an extended region of reduced wind speed downstream of a mountain. The dissipation of the kinetic energy of the flow of the wake may have taken place in breaking gravity waves or a hydraulic jump over the downslopes of the mountain, or elsewhere at the edges of the wake, referring to the last terms in Eq. (1), extended to all three dimensions. There may be a wake whether or not there is a downslope windstorm, and breaking waves. In fact, there are large, and extended wakes in flows with very high  $Nh/U$  with very little wave activity, and most of the flow diverted around the mountain, and not over the mountain. Dynamic aspects of mountain wakes, and how they relate to the ambient flow are discussed thoroughly in [Smith et al. \(1997\)](#), [Rotunno et al. \(1999\)](#), and [Epifanio and Rotunno \(2005\)](#), and aspects of the dissipation of kinetic energy, and the generation of potential vorticity associated with a mountain wake in stratified flows are presented comprehensively in [Schär and Smith \(1993\)](#), and idealized flows with bottom friction are addressed by [Grubišić et al. \(1995\)](#).

On the left side of the lower part of the diagram in [Fig. 1](#), there is close to geostrophic flow over a large mountain ridge. This flow is characterized by a geopotential ridge above a wide, and large mountain ridge. The classic paper presenting such a solution is [Queney \(1948\)](#), and a popular textbook description of the ridge is derived from conservation of potential vorticity on a rotating earth. This flow pattern is on quite a large scale, and is, in general, well reproduced by numerical models.

To the right, in the lower part of the diagram, we have low Rossby number flows, which are at the same time blocked on the upstream side of the mountain, and with a downstream wake. A relatively large proportion of the low-level flow is diverted to the left as it meets the mountain, and on this side, there is acceleration. There is flow stagnation on the upstream right flank of the mountain (facing downstream), but acceleration on the right hand side of the wake (still facing downstream). [Ólafsson \(2000\)](#) and [Petersen et al. \(2005\)](#) presented a collection of solutions of such asymmetric flows within the idealized framework. Classic examples of the upstream acceleration are the jet in southwesterly flows at Stad in W-Norway ([Barstad and Grønås, 2005](#); [Jonassen et al., 2012](#)), the Cape Tobin jet at E-Greenland ([Ólafsson et al.,](#)

2009), and the northeasterly flows to the southeast of Greenland (Moore and Renfrew, 2005; Ólafsson and Ágústsson, 2009; Petersen et al., 2009). An example of a much celebrated jet to the right hand side of the wake (facing downstream) is the Greenland tip jet, extending hundreds of kilometers to the east from the southernmost tip of Greenland (Cape Farewell) (Doyle and Shapiro, 1999; Petersen et al., 2003). A popular presentation of the asymmetry of the flow field is geostrophic adjustment to the pressure anomalies generated by the mountain. The upstream high accelerates the flow that is deviated to the left of the mountain, while the downstream low accelerates the jet emanating from the right hand edge of the mountain (facing downstream).

### 3 Forecasting the orographic flows

A primary requirement for accurately reproducing patterns of orographic flows in a numerical weather prediction model must be that the model reproduces the topography accurately. Needless to say, this depends highly upon the horizontal resolution of the model; if the model resolution is too coarse to reproduce a mountain, the flow pattern associated with that mountain will inevitably also be missed by the model. Coarse-resolution models tend to underestimate the height of mountains, unless the width of the mountains is much greater than the distance between grid points of the model. In such cases, the maximum wind speed in corner winds, and the minimum wind speed in wakes, and blockings are systematically underestimated by the models. This underestimation is particularly strong if each of the two worlds, the real world, and the model world fall into two different regimes, i.e., blocked, and nonblocked flows. The intensity of corner winds, gap winds, wakes, and blockings may also be sensitive to the steepness of the slopes. Consequently, too gentle slopes in a numerical model tend to lead to an underestimation of the magnitude of the acceleration or the deceleration of the flow in the respective regions.

Even though all relevant topographic elements are well resolved, there are still uncertainties that may be characterized as systematic. Assessing these uncertainties is important for interpreting the model output for forecasting, and may be useful for systematic assessment of uncertainties in the context of postprocessing the model output. These uncertainties may, in general, be classified in the following categories: regions of spatial gradients, flow close to the limits of regime changes (e.g., blocked to nonblocked flow), gravity waves, and hydraulic jump-like flows, and features with high temporal variability.

Regions of strong horizontal, and vertical gradients are in general preferred locations for uncertainties, due to uncertain position of the edges, and to some extent to uncertainties in the magnitude of the jets. A small change in the direction of the wind upstream of a mountain will, in most cases, lead to a similar shift in the position of the orographic flow pattern. Certain locations, close to the edges of regions of weak or strong winds, will move from being inside of a region of strong winds to entering a region of weak winds or vice versa. A typical error of this kind is when a given location at the outer edge of a wake moves between being inside the corner wind, or inside the wake. Fig. 4 shows an example of a wake, and jets emanating from the mountains of SE-Iceland in northerly winds. The two panels in Fig. 4 are output from a model simulation with an interval of 1 h. There are negligible changes in the upstream winds, but inside the encircled area on the downstream side, the wind speed increases from 5 to

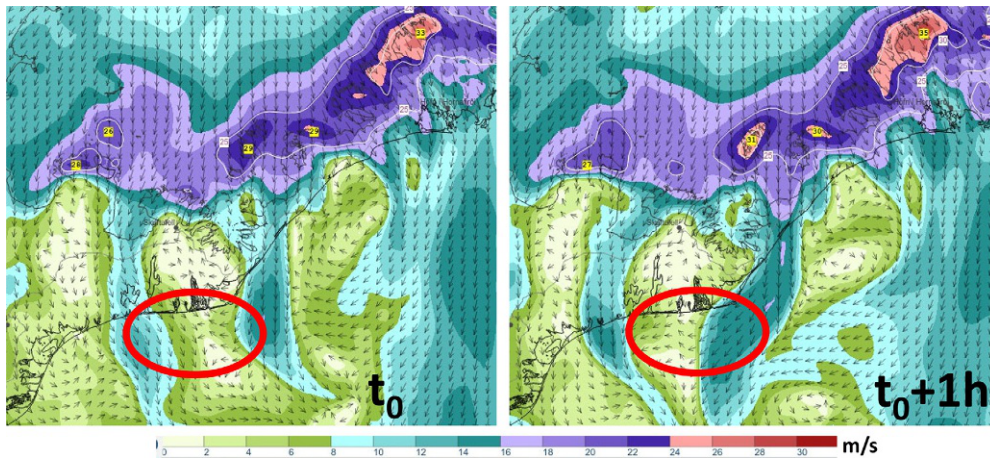


FIG. 4 Wind speed at 10 m (m/s) in the wake of the mountains of SE-Iceland in northerly flow over Iceland on 5 June 2020 at 05 and 06 UTC. An area with large temporal variability in the wake is encircled. The flow is simulated in real-time by the numerical model Harmonie operated by the Icelandic Meteorological Office and the Danish Meteorological Institute at a horizontal resolution of 2.5 km.

15 m/s in the eastern part of the area, while in the western part of the area, the wind speed is reduced from 13 to 3 m/s. These specific changes in wind pattern occur over the ocean, and they are hardly ever verified, but in cases like this, the model is unlikely to be consistently correct in time, and space. In the case of Fig. 4, the jets emanate from lowerings in the topography, and they are modulated by gravity waves to an uncertain extent. The vertical extent of wakes is typically less than the height of the mountain that generates the wake, and in the case of a shallow wake, the relatively strong winds above the wake may penetrate down to the surface, either by turbulent mixing or by vertical transport of momentum in gravity waves. This penetration may be very hard for numerical models to reproduce accurately, regardless whether it is driven by gravity waves or turbulent mixing, and even if the models were very capable of reproducing both the mixing, and the gravity waves, both processes may be very sensitive to both wind, and static stability, and a small change or error in either parameter may lead to large changes or errors in the flow.

At the limits of flow regimes, small changes in the upstream flow or small modifications of model calculations, such as in the treatment of turbulent mixing, may trigger a shift from one flow pattern or regime to another. Blocked flow with stagnation on the upstream side of a mountain, and a wake on the downstream side may thus enter the “flow over” regime with only little upstream deceleration, and no wake. Fig. 5 illustrates such a change; first, there is an upstream blocking (encircled), but an hour later, the blocking has disappeared, and yet there are only minor changes in the upstream wind field, and the static stability.

A multitude of aspects of gravity waves, including uncertainties in their generation, amplification, propagation, and breaking have been addressed by a very large number of authors in the scientific literature. There is no universal theory of gravity waves in a nonuniformly layered flow, and their simulation is still a challenge to numerical models. The waves are sensitive to changes in the profile of wind, and stability for at least certain values of both profiles at certain levels, depending on the mountain on which the flow impinges, and the properties

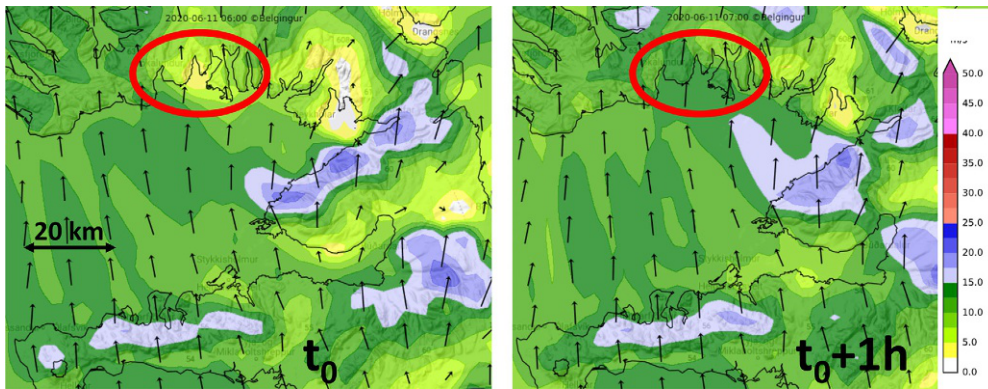


FIG. 5 Wind speed at 10m (m/s) in southerly flow over Iceland on 11 June 2020 at 06 and 07 UTC. An area with large temporal variability in the blocking upstream of the mountains of NW-Iceland is encircled. The flow is simulated in real-time by the numerical model WRF, operated by Belgingur Ltd. at a horizontal resolution of 3 km.

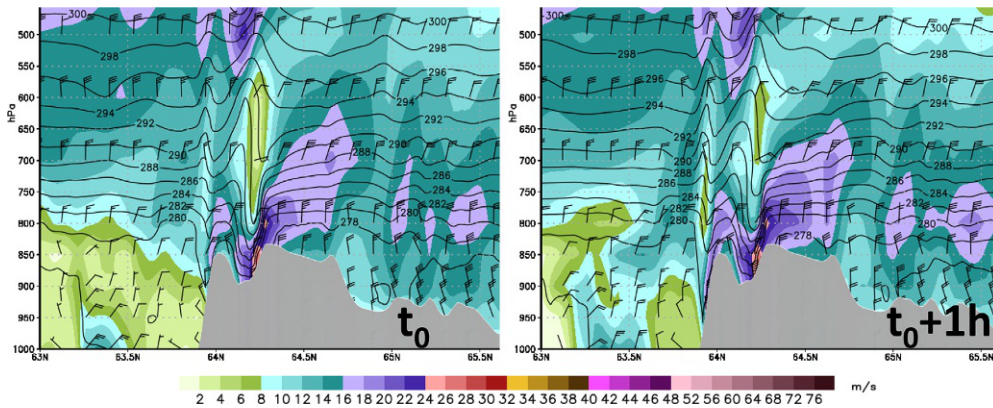


FIG. 6 Wind speed (m/s) and isentropes (K) in a S-N section across E-Iceland in northerly flow on 5 June 2020 at 15 and 16 UTC. The flow is simulated in real-time by the numerical model Harmonie operated by the Icelandic Meteorological Office and the Danish Meteorological Institute at a horizontal resolution of 2.5 km.

of the surface of the earth below the waves (e.g., [Jonassen et al., 2014](#)). They may also be sensitive to model details such as treatment of dissipation ([Doyle et al., 2000](#)) or even moisture ([Rögnvaldsson et al., 2011](#)). Even though many case studies appear to be able to reproduce the surface winds, and even parts of the wave pattern above, often after considerable tuning of tunable parameters of the numerical model, forecasting waves, and the associated downslope winds, remains a challenge. [Fig. 6](#) illustrates the large spatial and temporal variability of the flow associated with gravity waves. In only 1 h, the downslope surface winds increase dramatically and the wave pattern above has changed very much. Yet, there are no clear signs of changes in the upstream vertical profiles of wind and temperature [Reinecke and Durran \(2009\)](#) expressed this uncertainty in the following words concluding a study based on cases from the T-REX field campaign: “neither case suggests that much confidence should be



placed in the intensity of downslope winds forecast 12 or more hours in advance.” Fig. 7, which shows the performance operational high-resolution numerical forecasts with lead time of 24h, based on data from 2017 to 2019 is in line with this; there is very little predictive skill for cases of downslope winds, where either the predicted or the observed winds are above 15m/s.

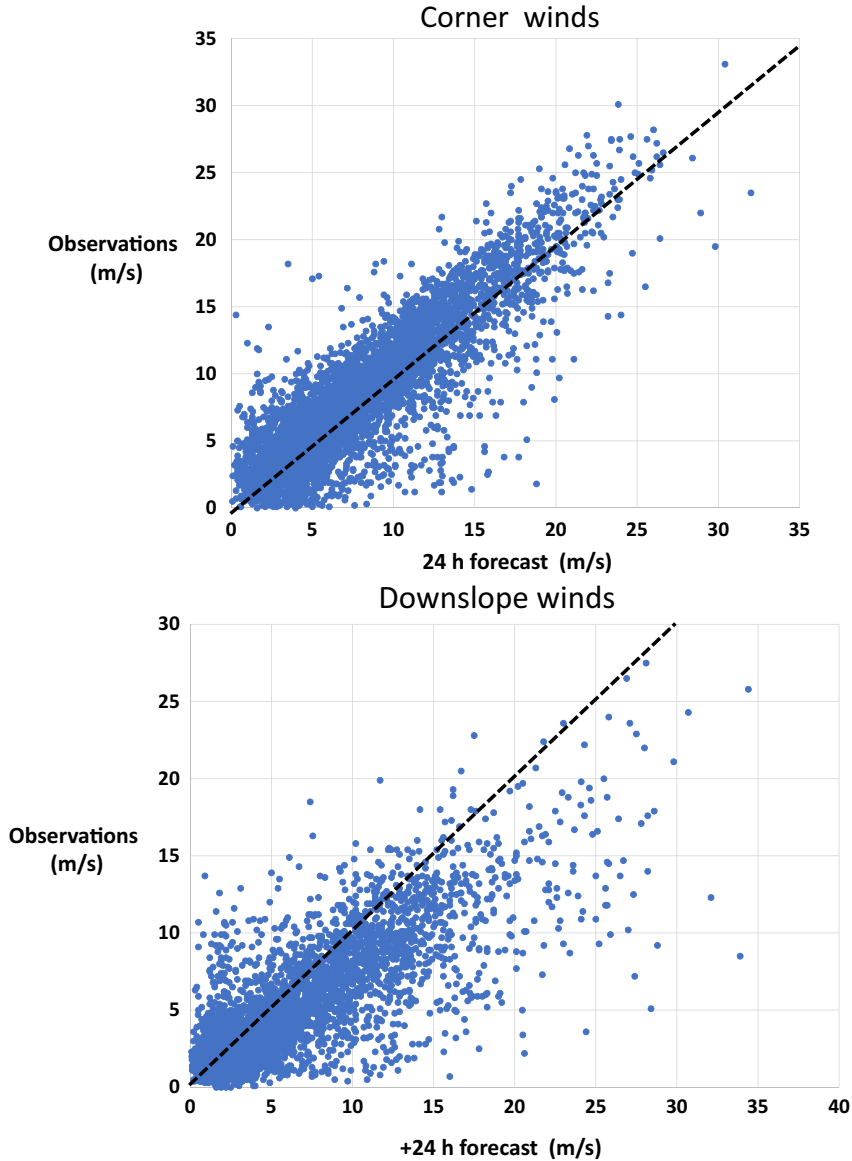
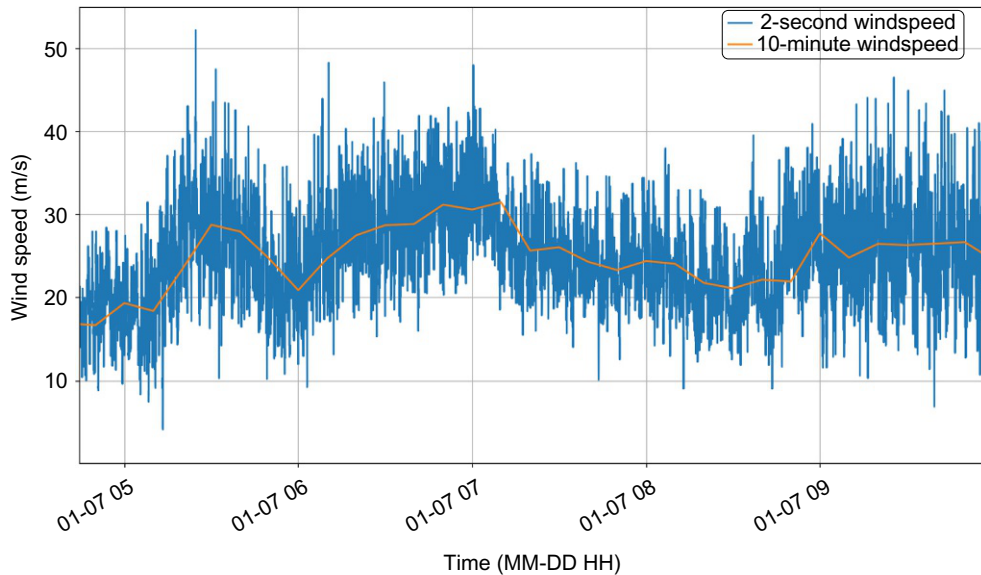


FIG. 7 Observed and forecasted (+24h) wind speed at Fagurhólmýri, SE-Iceland in winds from the NE (Corner winds) and at Kvísker, SE-Iceland in winds from the W or N (Downslope winds). The numerical forecast is from the operational suite of the model Harmonie at a horizontal resolution of 2.5km with initial and boundary conditions from the ECMWF.



**FIG. 8** Observations of surface wind speed at Kjalarnes, SW-Iceland on 7 January 2011 during a downslope windstorm. Data provided by the Icelandic Road Administration (Vegagerðin).

Temporal variability poses considerable uncertainty upon the forecasting of small-scale orographic flows, particularly on gravity waves, and downslope windstorms. High temporal variability of the winds is an integral part of gravity waves, and it is considered to be particularly important if the waves are breaking, as they go through phases of buildup, and breaking with large impacts on the surface wind speed. Turbulence is also associated with high temporal variability. Fig. 8 shows about 5 hours of instantaneous (2s) wind speed at the foothills of Mt. Esja in SW-Iceland during a downslope windstorm. The temporal variability is large on various time scales. There is definitely much turbulence, but one may assume that a part of the variability in Fig. 8, on the time scale of minutes to hours, is associated with gravity waves, either building up or breaking, and moving in space. Within the framework of shallow water, this may be expressed as variability associated with hydraulic jump-like flow features.

#### 4 Future improvements

General improvements in the assessment of initial, and boundary conditions as well as more sophisticated treatment of elements such as turbulence, and dissipation in numerical models can be expected to lead to improvements of the representation of the above details of mesoscale orographic flows. To the extent that increased resolution leads to improvements

in the representation of the topography, increased resolution may be expected to give better point forecasts. Apart from model issues such as representation of turbulence, and other boundary-layer processes, increased resolution tends to sharpen horizontal wind gradients, and may lead to fewer but bigger errors in regions with oscillating or uncertain position of the gradients.

In view of the sensitivity of gravity waves to the vertical profile of the atmosphere, improvements in vertical model resolution, and details in the initialization of features such as inversions, and vertical profile of winds will most likely lead to improvements in the forecasting of downslope windstorms.

## References

- Ágústsson, H., Ólafsson, H., 2010. The bimodal downslope windstorms at Kvísker. *Meteorol. Atmos. Phys.* 116, 27–42.
- Ágústsson, H., Ólafsson, H., 2014. Simulations of observed lee waves and rotor turbulence. *Mon. Weather Rev.* 142, 832–849.
- Baines, P.G., 1995. *Topographic Effects in Stratified Flows*. Cambridge University Press, New York, pp. 1–482.
- Barstad, I., Grønås, S., 2005. Southwesterly flows over southern Norway—mesoscale sensitivity to large-scale wind direction and speed. *Tellus A* 57 (2), 136–152.
- Belcher, S.E., Hunt, J.C.R., 1998. Turbulent flow over hills and waves. *Annu. Rev. Fluid Mech.* 30, 507–538.
- Doyle, J.D., Shapiro, M.A., 1999. Flow response to large-scale topography: the Greenland tip jet. *Tellus A* 5, 728–748.
- Doyle, J.D., Durran, D.R., Chen, C., Colle, B.A., Georgelin, M., Grubisic, V., Hsu, W.R., Huang, C., Landau, D., Lin, Y.L., Poulos, G.S., Sun, W.Y., Weber, D.B., Wurtele, M.G., Xue, M., 2000. An intercomparison of model-predicted wave breaking for the 11 January 1972. Boulder windstorm. *Mon. Weather Rev.* 128 (3), 901–914.
- Durran, D.R., 1990. Mountain waves and downslope winds. In: *Atmospheric Processes over Complex Terrain, Meteorological Monographs*, No. 45. American Meteorological Society, pp. 59–81.
- Epifanio, C.C., Rotunno, R., 2005. The dynamics of orographic wake formation in flows with upstream blocking. *J. Atmos. Sci.* 62 (9), 3127–3150. <https://doi.org/10.1175/JAS3523.1>.
- Gaberšek, S., Durran, D.R., 2004. Gap flows through idealized topography. Part I: forcing by large-scale winds in the nonrotating limit. *J. Atmos. Sci.* 61, 2846–2862.
- Gaberšek, S., Durran, D.R., 2006. Gap flows through idealized topography. Part II: effects of rotation and surface friction. *J. Atmos. Sci.* 63, 2720–2739.
- Grubišić, V., Smith, R.B., Schär, C., 1995. The effect of bottom friction on shallow-water flow past an isolated obstacle. *J. Atmos. Sci.* 52, 1985–2005.
- Hertenstein, R.F., Kuettner, J.P., 2005. Rotor types associated with steep lee topography: influence of the wind profile. *Tellus* 57A (2), 117–135.
- Jonassen, M.O., Ágústsson, H., Ólafsson, H., 2014. Impact of surface characteristics on flow over a mesoscale mountain. *Q. J. R. Meteorol. Soc.* 140, 2330–2341. <https://doi.org/10.1002/qj.2302>.
- Jonassen, M.O., Ólafsson, H., Reuder, J., Olseth, J.A., 2012. Multi-scale variability of winds in the complex topography of southwestern Norway. *Tellus* 64(11962) <https://doi.org/10.3402/tellusa.v64i0.11962>.
- Moore, G.W.K., Renfrew, I.A., 2005. Tip jets and barrier winds: a QuikSCAT climatology of high wind speed events around Greenland. *J. Clim.* 18, 3713–3725.
- Ólafsson, H., Bougeault, P., 1996. Nonlinear flow past an elliptic mountain ridge. *J. Atmos. Sci.* 53, 2465–2489.
- Ólafsson, H., 2000. The impact of flow regimes on asymmetry of orographic drag at moderate and low Rossby numbers. *Tellus* 52 (4), 365–379.
- Ólafsson, H., Ágústsson, H., 2009. Gravity wave breaking in easterly flow over Greenland and associated low level barrier- and reverse tip-jets. *Meteorol. Atmos. Phys.* 104, 191–197. <https://doi.org/10.1007/s00703-009-0024-9>.
- Ólafsson, H., Ágústsson, H., Shapiro, M.A., Kristjánsson, J.E., Barstad, I., Dörnbrack, A., 2009. The Cape Tobin jet. In: *Proc. Int. Conf. Alpine Meteorol., Raststatt, Germany*, pp. 224–225.
- Petersen, G.N., Kristjánsson, J.E., Ólafsson, H., 2005. The effect of upstream wind direction on atmospheric flow in the vicinity of a large mountain. *Q. J. R. Meteorol. Soc.* 131, 1113–1128.

- Petersen, G.N., Ólafsson, H., Kristjánsson, J.E., 2003. Flow in the lee of idealized mountains and Greenland. *J. Atmos. Sci.* 60, 2183–2195.
- Petersen, G.N., Renfrew, I.A., Moore, G.W.K., 2009. An overview of barrier winds off southeastern Greenland during the Greenland flow distortion experiment. *J. Atmos. Sci.* 135, 1950–1967.
- Queney, P., 1948. The problem of the airflow over mountains: a summary of theoretical studies. *Bull. Am. Meteorol. Soc.* 29, 16–26.
- Reinecke, P.A., Durran, D.R., 2009. Initial condition sensitivities and the predictability of downslope winds. *J. Atmos. Sci.* 66 (11), 3401–3418.
- Rögnvaldsson, Ó., Bao, J.W., Ágústsson, H., Ólafsson, H., 2011. Downslope windstorm in Iceland—WRF/MM5 model comparison. *Atmos. Chem. Phys.* 11, 103–120. <https://doi.org/10.5194/acp-11-103-2011>.
- Rotunno, R., Grubišić, V., Smolarkiewicz, P.K., 1999. Vorticity and potential vorticity in mountain wakes. *J. Atmos. Sci.* 16, 2796–2810.
- Schär, C., Smith, R.B., 1993. Shallow-water flow past isolated topography. 1. Vorticity production and wake formation. *J. Atmos. Sci.* 50, 1373–1400.
- Smith, R.B., 1985. On severe downslope winds. *J. Atmos. Sci.* 43, 2597–2603.
- Smith, R.B., 1989. Hydrostatic airflow over mountains. In: *Advances in Geophysics*, vol. 31. Academic Press, pp. 59–81.
- Smith, R.B., Gleason, A.C., Gluhosky, P.A., Grubišić, V., 1997. The wake of St. Vincent. *J. Atmos. Sci.* 54, 606–623.
- Smith, R.B., Grønås, S., 1993. Stagnation points and bifurcation in 3-D mountain airflow. *Tellus* 45, 28–43.
- Zängl, G., 2002. Stratified flow over a mountain with a gap: linear theory and numerical simulations. *Q. J. R. Meteorol. Soc.* 128, 927–949.